Periodica Polytechnica
Mechanical Engineering

Computer tomography based reconstruction of metal matrix syntactic foams

58(2), pp. 87-91, 2014
DOI:10.3311/PPme.7337

I. Kozma, *Ibolya* Zsoldos, *G.* Dorogi, *Sz.* Papp

RESEARCH ARTICLE

RECEIVED 06 FEBRUARY 2014; ACCEPTED AFTER REVISION 11 APRIL 2014

Abstract

In order to create 3D (three-dimensional) models for finite element calculations it is necessary to reconstruct the structure of metal foam composites reinforced by hollow ceramic spheres. A new algorithm was developed for this reconstruction work. This algorithm is based on the investigation of sphericity of the shapes found on CT (computer tomograph) layer records. Using this algorithm a 3D CAD (computer aided design) model of acceptable precision can be constructed.

Keywords

syntactic foam · CT based reconstruction

I. Kozma
Faculty of Mechanical Engineering, Széchenyi István University, Egyetem tér 1., H-9026 Győr, Hungary

Ibolya Zsoldos
Faculty of Mechanical Engineering, Széchenyi István University, Egyetem tér 1., H-9026 Győr, Hungary
email: zsoldos@sze.hu

G. Dorogi
Sz. Papp
Faculty of Mechanical Engineering, Széchenyi István University, Egyetem tér 1., H-9026 Győr, Hungary

1 Introduction

The metallic foams have a special class which satisfies the definition of particle reinforced metal matrix composites also. These are the metal matrix syntactic foams. The metal matrix syntactic foams have numerous perspective applications as covers, hulls, castings, or in automotive and electromechanical industry sectors because of their high energy absorbing and damping capability. In these porous materials the porosity is ensured by incorporating ceramic hollow microspheres [1]. The microspheres are commercially available and they contain mainly various oxide ceramics [2, 3].

The most important properties of the metal matrix syntactic foams are the compressive strength and the absorbed energy [4-10].

The quality and chemical composition of the microspheres influence many properties of the syntactic foams. And they have also strong influence during the production of the syntactic foams. The foams are usually produced by mixing technique and gravitational casting or by pressure infiltration [11-13].

Because of the strong effect of the quality of the microspheres (diameter of ~ 0.1-3 mm) on the mechanical and other properties of the foams the investigation of the structure of the syntactic foams is very important. In order to create real 3D models from the syntactic foams the CT-based reconstruction methods can be applicable. CT-based reconstruction methods are used successfully in many different materials research fields as for example porous polymeric materials (foams) [14], open celled and closed-cell metallic foams [15-16]. Recently the X-ray computed microtomography has been applied on porous fuel cell materials [17] and soil samples [18]. The history, the production, the geometrical, mechanical, thermal properties the dynamical behaviour and the fatigue processes of hollow spheres were studied in details [19].

Structural characterisation and morphology of metal foams were studied with models reconstructed from CT images [20]. In order to apply the CT-images for the reconstruction of the syntactic foams a new algorithm is shown in this work.

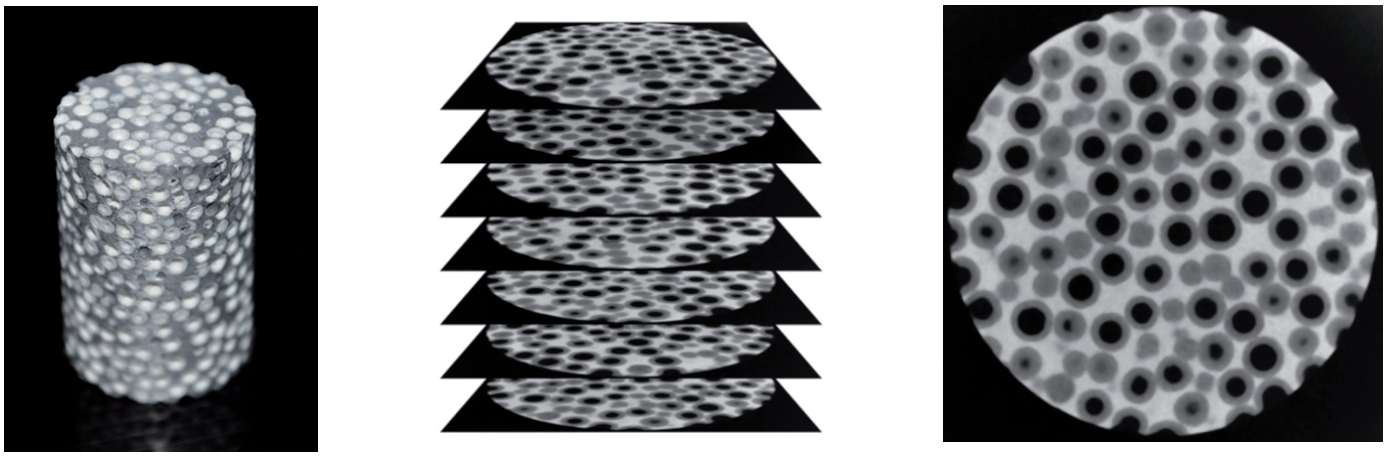

a b c

Fig. 1. a: Al composite sample reinforced by hollow ceramic spheres. **b:** CT layer records. **c:** One CT layer photographs.

2 Reconstruction algorithm

In this work our goal was to reconstruct the 3D structure of an Al composite sample reinforced by hollow ceramic spheres (radius range: 0.65-0.75 mm). The starting point was a specimen of a sample of the composite, a photograph is shown on Fig. 1.a. The size of the cylindrical specimen was Ø10x15 mm. The basis of the reconstruction was the CT analysis. Fig. 1.b shows some slices of the CT picture, one slice is shown in detail on Fig. 1.c. CT layer analysis was performed at the laboratory of the department of materials Science of Széchenyi István University, using a YXILON CT Modular type industrial CT equipment, using an X-ray tube of 225 kV, µfocus, with a resolution of 7 µm.

Software products offered for analyzing CT layer records (layer thickness of 7 µm) (e. g. Mimics, Geometry, YXlon CT software) can reconstruct detected air inclusions (e. g. bubbles in metal castings) as spheres. The number of the hollow spheres is 1309 in the specimen and the volume ratio of the ceramic hollow spheres in the specimen calculated by the software is 58%. This reconstruction, however, works with hollow ceramic spheres only on the internal surfaces; the reconstruction of the outer spherical surfaces is not yet solved. When analyzing the CT layer records it was observed that the wall thickness of the hollow ceramic spheres is not uniform (range of 0.2-0.3 mm), and it may also occur that the outer and internal spherical surfaces are not perfectly concentric. Furthermore, in several cases twin spheres (crossing each other) can also be found in the structure, which complicates the reconstruction further. Due to these problems we could not solve directly the full structure reconstruction problem using the standard CT handling and processing software. From the test data we could retrieve only the models of the internal spheres which were used in constructing the complete model of the composite.

In order to reconstruct the outer spheres we tried to find a solution by detecting circles on the CT layer records. For the detection of the circles first the Hough Circle algorithm was used. Fig. 2 shows a section of a hollow ceramic sphere. It can be seen that especially the outer contour is not a perfect circle. The Hough Circle algorithm [21] fits circles to more details of the contour resulting in several circles, see Fig. 2.b. In most cases, however, (as shown in Figure 1.b) none of these circles will be a best fitting circle of the outer contour. We have developed an algorithm to determine good fitting circles (in the case of the 3D model, spheres) which describe well the outer contour of the hollow spheres.

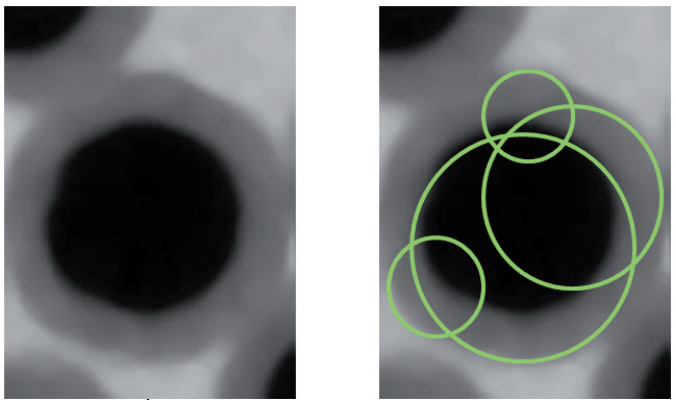

a b

Fig. 2. a: Detail of a CT layer record of a ceramic hollow sphere.
b: Circles fitted various arc portions.

The algorithm of sphericity

Several separate areas can be distinguished (segmented) from each other on a CT layer record. From these circular areas are sought for. As only the outer contours are to be detected, the area of the internal circles (see the black area in Fig. 2) is united with the area of the dark grey (area No. 1) sphere walls.

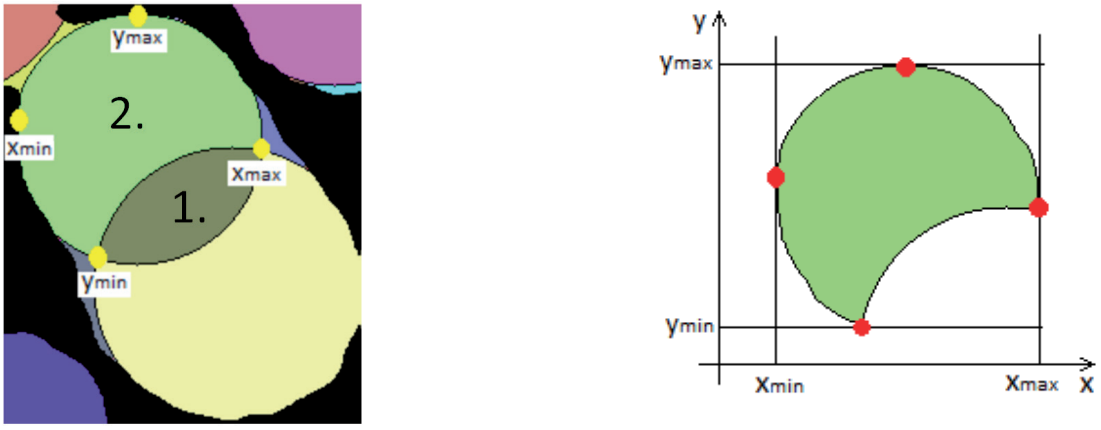

a b

Fig. 3. Determining the extreme coordinates used to characterize the sphericity of a given segmented area, shown by the example of the light green area (area No 2). (The detail is taken from the segmented areas on a CT layer record.)

In order to decide the sphericity of a certain shape the following two quantities are needed:

- The segmented area, T_S (e. g. Fig. 3.b), which is simply defined as the sum of the pixel areas belonging to the given area.
- Area of a circle, T_C defined by the extreme coordinates of the segmented area used to determine a circle radius (T_C is the area of the circle having radius of R_C).

$$R_C = \frac{\frac{y_{max} - y_{min}}{2} + \frac{x_{max} - x_{min}}{2}}{2} \tag{1}$$

The sphericity of a shape is defined as follows:

$$C = \frac{T_C}{T_S} 100\% \tag{2}$$

If the investigated shape is exactly a sphere, C will be 100%. If the shape of the segmented are deviates from a circle:

- if the deviation is slight C will be close to 100%,
- in the case of stronger deviation C will also be significantly differs form 100%.

In order to determine the sphericity more exactly the same segmented area was investigated also in rotated coordinate systems. In all rotated coordinate system a separate R_C value was determined and the T_C circular area was calculated form an average of these values. In this work the T_C value was calculated as an average from 36 pieces of values determined in coordinate systems rotated by 10°.

If the segmented areas are crossing circles (as e. g. the one shown by light green color (area No 2) in Fig. 2) the sphericity parameter, C will of course not approximate well 100%. Therefore the algorithm was completed by the following process:

Having determined the sphericity (C value) of a certain shape the adjacent segmented areas next to the given shape were identified. The union was taken with all these neighbors subsequently. If the calculated C value for the union was closer to 100% than the original C value, then the union was used instead of the original area. In Fig. 3 e. g. the union of the light green are with the neighboring grain-like grey area gives much better circle than the light green area itself. Thus we could solve also the problem of crossing circles (twin ceramic spheres).

The principle of sphericity is by itself very simple and can be programmed easily. In order to use it the areas should be properly segmented. For this the Hough Circle algorithm was used. It was observed that by using the Hough Circle algorithm is was possible to find circumscribed circles for each spherical wall section. From the plurality of circles shown in Fig. 4 around a section of the ceramic sphere wall that with the maximum radius was taken as the circumscribed sphere. Blue circles (1) sign matrix materials (false result), red circles (2) sign the hollow sphere walls in the cross-section and the green circles (3) contain the centre points of the hollow sphere.

Within the circumscribed spheres the RGB codes were used to identify the contiguous areas. During the test runs it was found that the R=G=B<130 filtering condition was acceptable to segment the various areas.

3 Running results, the CAD model

The determination of the sphere radius from two sections is shown in Fig. 5.

Using the notation of Fig. 5 the sphere radius, *r* can be calculated as follows:

$$r = \sqrt{\frac{\left[(a-b)^2 + h^2\right]\left[(a+b)^2 + h^2\right]}{4h^2}} \tag{3}$$

where *a* and *b* are the radii of the circles detected on two layer records and *h* is the distance between the layers.

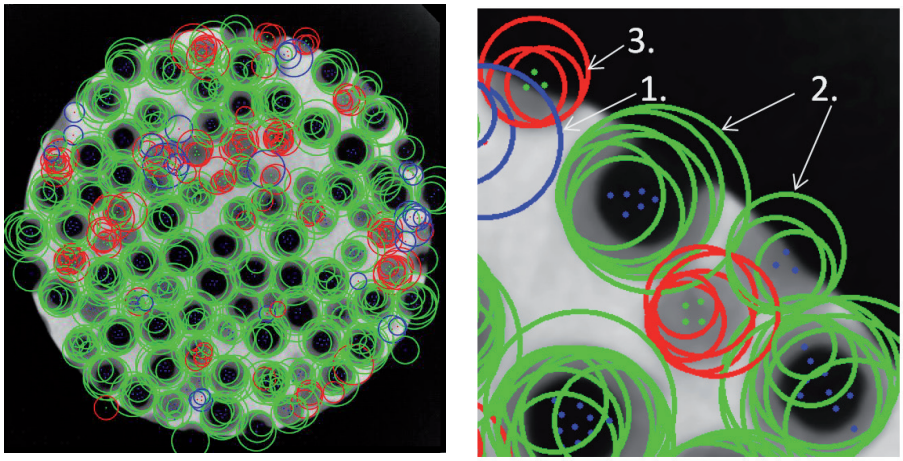

a b

Fig. 4. Searching for circumscribed sphere by the Hough Circle algorithm. **a:** one CT layer record. **b:** Detail from a CT layer record.

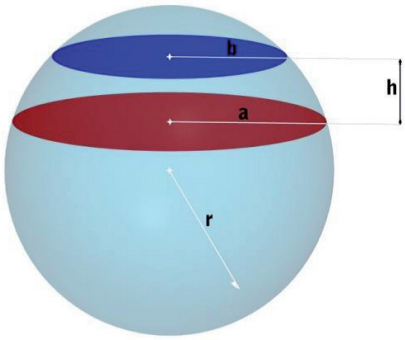

Fig. 5. Sphere parameters determined from the circles derived from layer records

For a given ceramic hollow sphere the data of the spherical wall were determined from the largest sections occurring at the central part.

1600 layer records were taken of the test specimen shown in Fig. 1. The circle detection algorithm was run on each layer record. From the data of the detected spheres a CAD model was constructed which allows running various engineering analyses (e. g. finite element calculations). The CAD model is shown in Fig. 6. To make the hollow spheres more conspicuous a model cut into two is presented.

4 Conclusion

Complete reconstruction of metal composites reinforced by ceramic hollow spheres from CT layer record cannot be performed using only standard CT image processing software. The algorithm of sphericity is useful for this purpose. Using this new algorithm a CAD model can be constructed even from specimens containing non-concentric or twin (crossing) spheres. With the help of the new algorithm running of the engineering analyses (e. g. tensile analysis) is possible on the reconstructed CAD models. Finite element models can be created using solid elements.

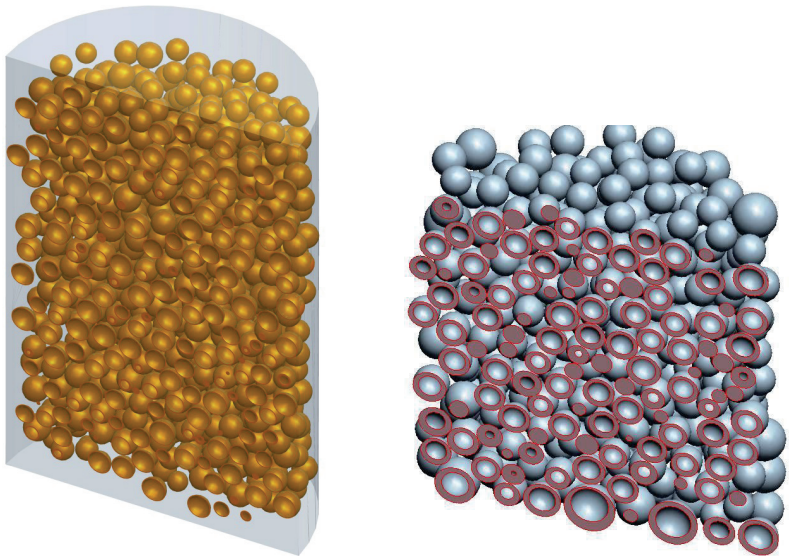

a b

Fig. 6. CAD models cut into two (a: with matrix, b: without matrix)

Acknowledgments

The research work presented in this paper/study/etc. was carried out as part of the TÁMOP-4.2.2.A-11/1/KONV-2012-0029 project in the framework of the New Széchenyi Plan. The realization of this project is supported by the European Union, and co-financed by the European Social Fund.

References

1 **Orbulov I. N., Dobránszky J.,** *Producing metal matrix syntactic foams by pressure infiltration.* Periodica Polytechnica Mechanical Engineering, 52 (1), pp. 35-42, (2008). DOI: 10.3311/pp.me.2008-1.06

2 **Envirospheres Ltd.,** http://www.envirospheres.com/products.asp, (Accessed 30.11.2011)

3 **Sphere Services Inc.,** http://www.sphereservices.com/ (Accessed 30.11.2011)

4 **Wu G. H., Dou Z. Y., Sun D. L., Jiang L.T., Ding B. S., He B. F.,** *Compression behaviors of cenosphere–pure aluminum syntactic foams.* Scripta Materialia, 56 (3), pp. 221-224, (2007). DOI: 10.1016/j.scriptamat.2006.10.008

5 **Orbulov I. N., Ginsztler J.,** *Compressive characteristics of metal matrix syntactic foams.* Composites Part A: Applied Science and Manufacturing, 43 (4), pp. 553-561, (2012). DOI: 10.1016/j.compositesa.2012.01.008

6 **Orbulov I. N., Májlinger K.,** *Microstructural aspects of ceramic hollow microspheres reinforced metal matrix composites.* International Journal of Materials Research, 104 (9), pp. 903-911, (2013). DOI: 10.3139/146.110944

7 **Rohatgi P. K., Kim J. K., Gupta N., Alaraj S., Daoud A.,** *Compressive characteristics of A356/fly ash cenosphere composites synthesized by pressure infiltration technique.* Composites Part A: Applied Science and Manufacturing, 37 (3), pp. 430-437, (2006). DOI: 10.1016/j.compositesa.2005.05.047

8 **Palmer R. A., Gao K., Doan T. M., Green L., Cavallaro G.,** *Pressure infiltrated syntactic foams—Process development and mechanical properties.* Materials Science and Engineering: A, 464 (1-2), pp. 85-92, (2007). DOI: 10.1016/j.msea.2007.01.116

9 **Balch D. K., O'Dwyer J. G., Davis G. R., Cady C. M., Gray III G. T., Dunand D. C.,** *Plasticity and damage in aluminum syntactic foams deformed under dynamic and quasi-static conditions.* Materials Science and Engineering: A, 391 (1-2), pp. 408-417, (2005). DOI: 10.1016/j.msea.2004.09.012

10 **Drury W. J., Rickles S. A., Sanders T. H., Cochran J. K.,** *Light weight alloys for aerospace applications.* The Minerals Metals and Materials Society 1998, 311-322.

11 **Rohatgi P. K., Guo R. Q., Iksan H., Borchelt E. J., Asthana R.,** *Pressure infiltration technique for synthesis of aluminum–fly ash particulate composite.* Materials Science and Engineering: A, 244 (1), pp. 22-30, (1998). DOI: 10.1016/S0921-5093(97)00822-8

12 **Bárczy T., Kaptay Gy.,** *Modelling the infiltration of liquid metals into porous ceramics.* Materials Science Forum, Vol. 473-474, pp. 297-302, (2005).

13 **Trumble P. K.,** *Spontaneous infiltration of non-cylindrical porosity: Close-packed spheres.* Acta Materialia, 46 (7), pp. 2363-2367, (1998). DOI: 10.1016/S1359-6454(98)80017-7

14 **Léonard A., Calberg C., Kerckhofs G., Wevers M., Jérôme R., Pirard J. P., Germain A., Blacher S.,** *Characterization of the porous structure of biodegradable scaffolds obtained with supercritical CO_2 as foaming agent.* Journal of Porous Materials, 15 (4), pp. 397-403 (2008). DOI: 10.1007/s10934-006-9094-y

15 **Vicente J., Topin F., Daurelle J-V.,** *Open Celled Material Structural Properties Measurement: From Morphology To Transport Properties.* Materials Transactions, 47 (9), pp. 2195-2202, (2006).

16 **Jeon I., Katou K., Sonoda T., Asahina T., Kang K. J.,** *Cell wall mechanical properties of closed-cell Al foam.* Mechanics of Materials 41 (1), pp.60-73, (2009). DOI: 10.1016/j.mechmat.2008.08.002

17 **Wargo E. A., Kotaka T., Tabuchi Y., Kumbur E. C.,** *Comparison of focused ion beam versus nano-scale X-ray computed tomography for resolving 3-D microstructures of porous fuel cell materials.* Journal of Power Sources, 241, pp. 608-618, (2013). DOI: 10.1016/j.jpowsour.2013.04.153

18 **Houston A. N., Schmidt S., Tarquis A. M., Otten W., Baveye P. C., Hapca S. M.,** *Effect of scanning and image reconstruction settings in X-ray computed microtomography on quality and segmentation of 3D soil images.* Geoderma, 207-208, pp. 154-165, (2013). DOI: 10.1016/j.geoderma.2013.05.017

19 **Oechsner A., Augustin C.,** *Multifunctional Metallic Hollow Sphere Structures*. Springer (2009).

20 **Vesenjak M., Borovinšek M, Fiedler T., Higa Y., Ren Z.,** *Structural characterisatition of advanced pore morphology (APM) foam elements*. Materials Letters, 110, pp. 201-203, (2013). DOI: 10.1016/j.matlet.2013.08.026

21 **Yuen H. K., Princen J., Illingworth J., Kittler J.,** *Comparative study of Hough Transform methods for circle finding.* Image and Vision Computing, 8 (1), pp. 71-77, (1990). DOI: 10.1016/0262-8856(90)90059-